Ground and excited states of a bound polaron in a purely two-dimensional quantum well

1991 J. Phys.: Condens. Matter 3 9401

(http://iopscience.iop.org/0953-8984/3/47/013)

J. Phys.: Condens. Matter 3 (1991) 9401–9416. Printed in the UK

Ground and excited states of a bound polaron in a purely two-dimensional quantum well

Shreekantha Sil† and Ashok Chatterjee‡

† Solid State and Molecular Physics Division, Saha Institute of Nuclear Physics, Sector 1, Block AF, Bidhannagar, Calcutta 700 064, India

‡ School of Physics, University of Hyderabad, Central University PO, Hyderabad 500 134, India

Received 28 November 1990, in final form 1 July 1991

Abstract. The bound-polaron problem in a purely two-dimensional quantum well is studied variationally for the entire range of the electron–phonon coupling constant and the Coulomb binding parameter. The ground-state energy, the average number of virtual phonons around the electron and the size of the polaron are calculated. A comparison made with the corresponding quantities for bulk crystals shows that the polaronic effects are more pronounced in two dimensions. The energies of the first two excited states are obtained and the phonon-induced Lamb shift corrections are computed for several polar materials.

1. Introduction

With the development of modern fabrication techniques like molecular-beam epitaxy and metal–organic chemical-vapour deposition, it has now become possible to realize electron systems in quasi one or two dimensions. Consequently, much effort (see [1] for references) has lately gone into exploring electronic states at surfaces and interfaces and in quantum wells and heterojunction superlattices of polar semiconductors. These studies are important from the point of view of device technology and also for the understanding of a number of surface phenomena such as transport properties in thin films, photoemission and electron diffraction. For the quantum-well problem, both purely two-dimensional (2D) and quasi-two-dimensional polaron models have been studied and one of the most interesting results emerging from the free surface optical (SO) polaron model is that the polaronic properties are more pronounced in two dimensions than in three dimensions.

Bhattacharya *et al* [2] have introduced the model problem of an extrinsic quasi-2D electron interacting with the SO phonons of a polar material and a positive Coulomb impurity localized at the surface. Imperfections being a rule rather than an exception, such an impurity-bound 2D polaron is obviously more realistic and is therefore of much practical importance. Gu and his collaborators [3] have considered in a series of papers the case of an intrinsic bound polaron localized at surfaces and interfaces of polar materials and in polar slabs. Their work has revealed several interesting features about these systems. Mason and Das Sarma [4] have calculated the phonon-induced shifts in shallow donor levels in semiconductor quantum structures such as $Al_xGa_{1-x}As$–GaAs

0953-8984/91/479401 + 16 $03.50

quantum wells and the CdTe–HgTe system using a purely 2D polaron model and have shown that the phonon Lamb shifts obtained perturbatively are negligibly small. Very recently, the ground state (GS) of this model has been studied in the limiting cases by Bhattacharya *et al* [5], who have also proposed a new dimensional scaling relation for the GS energy. In the present paper we address ourselves to the same 2D model quantum-well problem for the entire range of coupling parameters. Using a variant of the Lee, Low and Pines (LLP) method [6] as proposed by Huybrechts (LLP-H) [7], we obtain the GS energy, the size of the polaron, the average number of virtual phonons in the polaron cloud and the first two internal excited-state energies. To examine the efficacy of this method we also extend the path-integral calculation of [5] in the harmonic oscillator effective potential approximation to all coupling and compare with the corresponding LLP-H GS results.

2. The model Hamiltonian

The model we consider is as follows. The material under study is an extremely thin film of an ionic crystal or a polar semiconductor on a non-polar substrate, and for simplicity it is modelled by a purely 2D quantum well. The material contains an extra electron at the bottom of its conduction band which interacts with the (2D) optical phonons of the system. Let us also consider a localized Coulomb impurity in the system which can bind the electron. Assuming the effective-mass approximation to be valid the Hamiltonian for such a purely 2D electron–impurity system interacting with 2D optical phonons of the polar medium may be written as

$$H' = -\frac{\hbar^2}{2m}\nabla_{\rho'}^2 - \frac{e^2}{\bar{\varepsilon}_\infty \rho'} + \hbar\omega_s \sum_{q'} (\tilde{b}_{q'}^\dagger \tilde{b}_{q'} + \tfrac{1}{2}) + \sum_{q'} [\xi_{q'}' (e^{-iq'\cdot\rho'} - 1)\tilde{b}_{q'}^\dagger + \text{HC}] \qquad (2.1)$$

where all vector are two-dimensional and $\rho'^2 = x'^2 + y'^2$. The first term refers to the kinetic energy of the electron in two dimensions; the second term describes the electron impurity interaction, where $\bar{\varepsilon}_\infty$ is an effective dielectric constant given by

$$\bar{\varepsilon}_\infty = (\varepsilon_\infty + 1)/2 \qquad (2.2)$$

ε_∞ being the high-frequency dielectric constant of the material; the third term is the unperturbed 2D optical phonon Hamiltonian, with ω_s denoting the dispersionless optical phonon frequency in two dimensions; and the fourth term gives the electron–phonon interaction as well as the impurity–phonon coupling, the impurity being considered to be centred at the origin. The coefficient $\xi_{q'}'$ is given by

$$\xi_{q'}' = 2\pi i \left(\frac{\hbar e^2}{2\delta A' \omega_s}\right)^{1/2} \frac{1}{q'} \qquad (2.3)$$

where A' measures the area of the surface,

$$\delta = 2\pi/[\omega_s^2 (E_s - E_\infty)] \qquad (2.4)$$

$$E_s = (\varepsilon_s - 1)/(\varepsilon_s + 1) \qquad (2.5)$$

$$E_\infty = (\varepsilon_\infty - 1)/(\varepsilon_\infty + 1) \qquad (2.6)$$

ε_s being the static dielectric constant of the medium. We shall work in the Feynman units and therefore scale the energy by $\hbar\omega_s$, length by u^{-1}, where u is given by

$\hbar^2u^2/m = \hbar\omega_s$, area by u^{-2} and wavevectors by u. The Hamiltonian (2.1) then reduces to the following dimensionless form:

$$H = \frac{H'}{\hbar\omega_s} = -\tfrac{1}{2}\nabla_\rho^2 - \frac{\beta}{\rho} + \sum_q (\tilde{b}_q^\dagger \tilde{b}_q + \tfrac{1}{2}) + \sum_q [\xi_q(e^{-iq\cdot\rho} - 1)\tilde{b}_q^\dagger + \text{HC}] \tag{2.7}$$

where

$$\xi_q = i(\sqrt{2}\,\pi\alpha/qA)^{1/2} \tag{2.8}$$

$$\alpha = e^2(E_s - E_\infty)(m/2\hbar^2\omega_s)^{1/2} \tag{2.9}$$

$$\beta = \frac{e^2}{\hbar\omega_s\varepsilon}\left(\frac{\hbar}{m\omega_s}\right)^{-1/2} \tag{2.10}$$

α and β being dimensionless coupling parameters. The impurity–phonon interaction term can, however, be completely eliminated by performing the canonical transformation [8]:

$$b_q = \tilde{b}_q - \xi_q. \tag{2.11}$$

Finally ignoring an infinite constant energy $(\Sigma_q|\xi_q|^2)$, which is equivalent to adjusting the baseline of the energy, the system Hamiltonian can be expressed as

$$H = -\tfrac{1}{2}\nabla_\rho^2 - \frac{\beta}{\rho} + \sum_q (b_q^\dagger b_q + \tfrac{1}{2}) + \sum_q (\xi_q e^{-iq\cdot\rho} b_q^\dagger + \text{HC}) \tag{2.12}$$

where β is the renormalized Coulomb binding parameter given by

$$\beta = \frac{e^2}{\hbar\omega_s\bar{\varepsilon}_s}\left(\frac{\hbar}{m\omega_s}\right)^{-1/2} \tag{2.13}$$

with

$$\bar{\varepsilon}_s = (\varepsilon_s + 1)/2. \tag{2.14}$$

3. The ground state

In the LLP-H method the first LLP transformation [6] is modified as

$$U_1 = \exp\left(-ia\sum_q q\cdot r b_q^\dagger b_q\right) \tag{3.1}$$

where a is a variational parameter. Then after the second LLP transformation [6]

$$U_2 = \exp\left(\sum_q f_q b_q^\dagger - f_q^* b_q\right) \tag{3.2}$$

the Hamiltonian (2.12) becomes

$$\tilde{H} = U_2^{-1}U^{-1}HU_1U_2 \tag{3.3}$$

$$= \tfrac{1}{2}\nabla_\rho^2 - \frac{\beta}{\rho} + \sum_q (1 + a^2q^2/2)(b_q^\dagger + f_q^*)(b_q + f_q)$$

$$+ \sum_q [\xi_q e^{-i(1-a)q\cdot\rho}(b_q^\dagger + f_q^*) + \text{HC}] - a\sum_q p\cdot q(b_q^\dagger + f_q^*)(b_q + f_q)$$

$$+\frac{a^2}{2}\sum \boldsymbol{q}\cdot\boldsymbol{q}'(b_q^\dagger + f_q^*)(b_{q'} + f_{q'}^*)(b_{q'} + f_{q'})(b_q + f_q) \tag{3.4}$$

where $\boldsymbol{p}$ is the electron momentum and the function f_q is to be obtained variationally. When $a = 1$ this modified procedure reduces to the usual LLP method, and for $a = 0$ this scheme is equivalent to the Landau–Pekar formalism. The variational energy is now written as

$$E = \langle\Phi(\boldsymbol{\rho})|\langle 0|\tilde{H}|0\rangle|\Phi(\boldsymbol{\rho})\rangle \tag{3.5}$$

where $\Phi(\boldsymbol{\rho})$ is the electronic function to be chosen variationally and $|0\rangle$ is the unperturbed zero-phonon state. If we assume that f_q is a function of $|\boldsymbol{q}|$ only, then

$$\sum_q \boldsymbol{q}|f_q|^2 = 0 \tag{3.6}$$

and the variational energy simplifies to

$$E = \langle\Phi|(-\tfrac{1}{2}\nabla_\rho^2 - \beta/\rho)|\Phi\rangle + \sum_q (1 + a^2q^2/2)|f_q|^2 + \sum_q (\xi_q\rho_q^* f_q^* + \text{HC}) \tag{3.7}$$

where

$$\rho_q = \langle\Phi(\boldsymbol{\rho})|e^{i(1-a)\boldsymbol{q}\cdot\boldsymbol{\rho}}|\Phi(\boldsymbol{\rho})\rangle \tag{3.8}$$

is the Fourier transform of the renormalized charge density. Minimizing (3.7) with respect to f_q^* now yields

$$f_q = -\xi_q\rho_q^*/(1 + a^2q^2/2) \tag{3.9}$$

$$E = \langle\Phi(\boldsymbol{\rho})|(-\tfrac{1}{2}\nabla_\rho^2 - \beta/\rho)|\Phi(\boldsymbol{\rho})\rangle - \sum_q \frac{|\xi_q|^2|\rho_q|^2}{(1 + a^2q^2/2)}. \tag{3.10}$$

The mean number of virtual phonons N in the cloud around the electron in the GS may be written as

$$N = \langle\Phi(\boldsymbol{\rho})|\langle 0|\tilde{N}|0\rangle|\Phi(\boldsymbol{\rho})\rangle = \sum_q |f_q|^2 \tag{3.11}$$

where

$$\tilde{N} = U_2^{-1}U_1^{-1}b_q^\dagger b_q U_1 U_2 \tag{3.12}$$

and the size of the polaron R may be defined as

$$R = \langle\Phi(\boldsymbol{\rho})|\rho|\Phi(\boldsymbol{\rho})\rangle. \tag{3.13}$$

So far the electronic wavefunction has not been specified. Now we shall consider two types of trial wavefunctions, namely the Guassian function (the harmonic-oscillator approximation) and the Coulomb 1s function (the hydrogenic approximation).

3.1. The harmonic-oscillator approximation

Choosing

$$\Phi(\boldsymbol{\rho}) = (\lambda/\sqrt{\pi})\exp(-\lambda^2\rho^2/2) \tag{3.14}$$

we obtain

$$\rho_q = \exp[-(1-a)^2q^2/(4\lambda^2)]. \tag{3.15}$$

Equations (3.10), (3.11) and (3.13) then reduce to

$$E = \frac{\lambda^2}{2} - \sqrt{\pi}\,\beta\lambda - \frac{\pi\alpha}{2}\exp\left(-\frac{(1-a)^2}{a^2\lambda^2}\right)\operatorname{erfc}\left(\frac{(1-a)}{a\lambda}\right) \tag{3.16}$$

$$N = \frac{\alpha}{\sqrt{2}}\int \mathrm{d}q\,\frac{\exp[-(1-a)^2q^2/(2\lambda^2)]}{(1+a^2q^2/2)^2} \tag{3.17}$$

$$R = \sqrt{\pi}/(2\lambda) \tag{3.18}$$

where $\operatorname{erfc}(x)$ is the complementary error function. Minimization of (3.16) with respect to λ now gives

$$\lambda = \sqrt{\pi}\,\beta + (\pi/2)\alpha t\,\mathrm{e}^{t^2}\operatorname{erfc}(t) \tag{3.19}$$

$$E = -\tfrac{1}{2}[\sqrt{\pi}\,\beta + (\pi\alpha t/2)\,\mathrm{e}^{t^2}\operatorname{erfc}(t)]^2 - (\pi\alpha/2)\,\mathrm{e}^{t^2}\operatorname{erfc}(t) \tag{3.20}$$

$$N = \frac{\alpha}{\sqrt{2}}\int \mathrm{d}q\,\exp\left(\frac{-(1-a)^2q^2}{2[\sqrt{\pi}\,\beta + (\pi/2)\alpha t\,\mathrm{e}^{t^2}\operatorname{erfc}(t)]}\right)\left(1+\frac{a^2q^2}{2}\right)^{-2} \tag{3.21}$$

$$R = \sqrt{\pi}/2[\sqrt{\pi}\,\beta + (\pi/2)\alpha t\,\mathrm{e}^{t^2}\operatorname{erfc}(t)] \tag{3.22}$$

where

$$t = (1-a)/a\lambda \tag{3.23}$$

is to be treated as a new variational parameter instead of a. The GS energy is finally obtained by minimizing (3.20) with respect to t. With this variationally obtained value of t we can then calculate the number of phonons and the size of the polaron from (3.21) and (3.22) respectively. For all values of α and β, calculation has to be performed numerically. However, in the limiting cases it is possible to get analytical expressions.

(i) Weak-coupling weak-binding (extended-state) limit ($\alpha \to 0$, $\beta \to 0$, $a \to 1$). In this limit

$$E = -\pi\alpha/2 - \pi\beta^2/2 \tag{3.24}$$

$$N = \pi\alpha/4 \tag{3.25}$$

$$R = 1/(2\beta). \tag{3.26}$$

It is interesting to note that in the extended-state (ES) limit the average number of phonons depends on the electron–phonon coupling only, while the size of the polaron is governed by the impurity binding parameter.

(ii) Localized-state (LS) limit ($a \to 0$). In this limit, $t \to \infty$ and we use the asymptotic relation

$$\sqrt{\pi}\,t\,\mathrm{e}^{t^2}\operatorname{erfc}(t) = 1. \tag{3.27}$$

The GS energy is then obtained as

$$E = -(\pi/8)(\alpha + 2\beta)^2 \tag{3.28}$$

which is the Landau–Pekar result [5]. The average number of phonons and the polaron size are given by

$$N = (\pi/4)\alpha(\alpha + 2\beta) \tag{3.29}$$

$$R = 1/(\alpha + 2\beta) \tag{3.30}$$

which in contrast to the weak-coupling case now depend on both the electron–phonon coupling constant and the Coulomb binding parameter.

3.2. The hydrogenic approximation

In this case we take the trial function to be the GS of a 2D hydrogenic atom:

$$\Phi(\boldsymbol{\rho}) = 2^{2/3}(\gamma/\sqrt{\pi})\, e^{-2\gamma\rho} \tag{3.31}$$

where γ is a variational parameter. The renormalized charge density is now given by

$$\rho_q = [1 + (1-a)^2 q^2/(16\gamma^2)]^{-3/2} \tag{3.32}$$

so that equations (3.10), (3.11) and (3.13) reduce to

$$E = 2\gamma^2 - 4\gamma\beta - (1 + \sqrt{2}\,\gamma t')F(t') \tag{3.33}$$

$$N = (1 + \sqrt{2}\,\gamma t')G(t') \tag{3.34}$$

$$R = 1/(2\gamma) \tag{3.35}$$

where

$$t' = (1-a)/(\sqrt{2}\,a\gamma) \tag{3.36}$$

$$F(t') = (\alpha\pi/8)(3t'^2 + 18t' + 32)/(t'+2)^3 \tag{3.37}$$

$$G(t') = (\alpha\pi/8)(3t'^3 + 24t'^2 + 64t' + 32)/(t'+2)^4. \tag{3.38}$$

Minimization of (3.33) with respect to γ now leads to

$$\gamma = \beta + (\sqrt{2}/4)t'F(t') \tag{3.39}$$

and we have

$$E = -2[\beta + (\sqrt{2}/4)t'F(t')]^2 - F(t') \tag{3.40}$$

$$N = [1 + \sqrt{2}\,\beta t' + (t'^2/2)F(t')]G(t') \tag{3.41}$$

$$R = 1/\{2[\beta + (\sqrt{2}/4)t'F(t')]\} \tag{3.42}$$

where t' is to be obtained from

$$\delta E/\delta t' = 0. \tag{3.43}$$

In the ES limit we obtain

$$E = -2\beta^2 - \pi\alpha/2 \tag{3.44}$$

$$N = \pi\alpha/4 \tag{3.45}$$

$$R = 1/(2\beta) \tag{3.46}$$

while in the LS limit the results are

$$E = -2[\beta + 3\pi\alpha/(16\sqrt{2})] \tag{3.47}$$

$$N = (3\sqrt{2}\,\pi\alpha/8)[\beta + 3\pi\alpha/(16\sqrt{2})] \tag{3.48}$$

$$R = 2[\beta + 3\pi\alpha/(8\sqrt{2})]^{-1}. \tag{3.49}$$

Again for all values of the coupling parameters calculation has to be performed numerically. The numerical results are summarized below.

3.3. Numerical results

In both harmonic-oscillator and hydrogenic approximations, we have studied the α dependence of E, N and R over the entire range of α numerically for two values of β

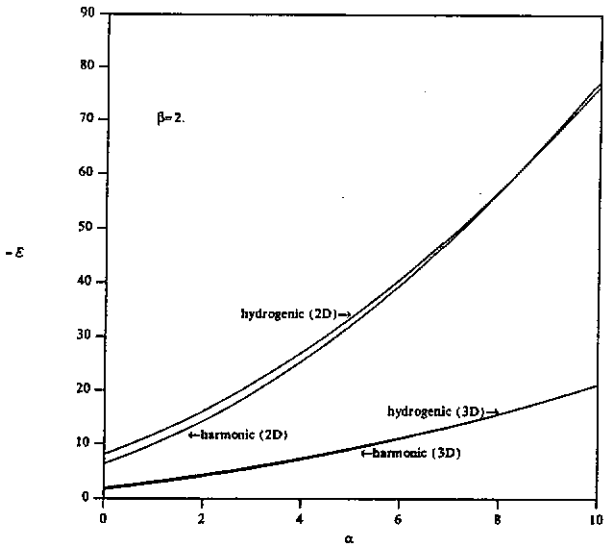

Figure 1. The GS energy E (in Feynman units) versus α for $\beta = 2$ in two and three dimensions in harmonic-oscillator and hydrogenic approximations.

($\beta = 2$ and $\beta = 10$). Results are shown graphically in figures 1 to 6 where we also plot the corresponding bulk (3D) values for comparison.

In figure 1 we show the plot of the 2D and 3D GS energies versus α for $\beta = 2$. For the same value of α the bound polaron in a quantum well clearly has a lower energy than in a bulk crystal. Also the difference between the 2D and 3D energies appears to increase monotonically with α. It is furthermore observed that, for small values of α, the hydrogenic trial function gives lower results in both 2D and 3D. However, for large α, the harmonic-oscillator approximation turns out to be a better approximation. This is clearly evident for the quantum-well case, for which the two curves corresponding to the two types of trial wavefunctions cross each other at about $\alpha = 8.5$. For the bulk problem, on the other hand, our figure does not show any such crossing. However, we guess that the crossing in this case will probably occur at some higher value of α. Moreover if β is small, the crossing may be expected at a smaller value of α.

Figure 2 gives the plot of the GS energy for $\beta = 10$. Again the energy is lower in 2D. Interestingly, however, now for the entire range of α the hydrogenic approximation yields lower results in both 2D and 3D and no indication of aforementioned crossing is observed. Thus, when α and β are both large or both small or when α is small and β is large, the hydrogenic wavefunction provides better answers for the GS energy, while in the case of small β and large α the effective potential for the electron's motion is better approximated by the harmonic-oscillator potential. It is furthermore observed that the scaling relation between the 2D and 3D bound-polaron energies

$$E^{2D} = \tfrac{2}{3}E^{3D}(\tfrac{3}{4}\pi\alpha, \tfrac{3}{4}\pi\beta) \tag{3.50}$$

which was proposed by Bhattacharya *et al* [5] in the harmonic-oscillator approximation within the Feynman–Haken path-integral formalism is also satisfied in the LLP-H scheme (again in the harmonic-oscillator approximation only) for the entire range of α and β.

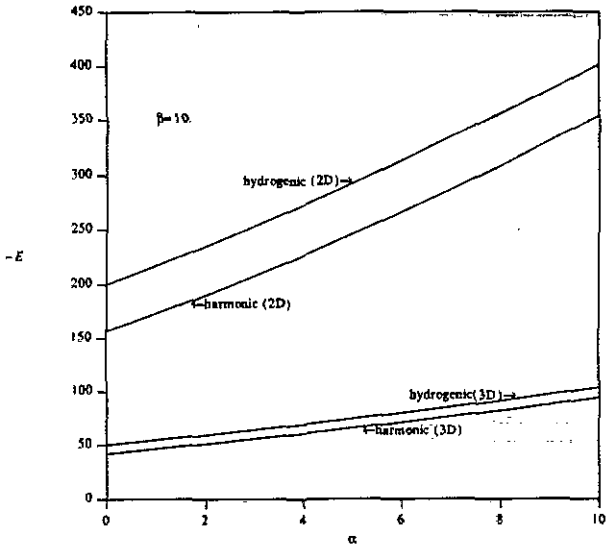

Figure 2. The GS energy E (in Feynman units) versus α for $\beta = 10$ in two and three dimensions in harmonic-oscillator and hydrogenic approximations.

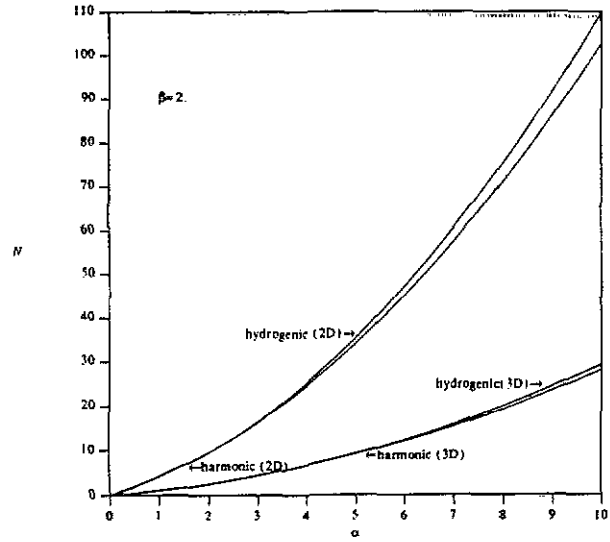

Figure 3. Average number of phonons N around the electron in the GS versus α for $\beta = 2$ in two and three dimensions in harmonic-oscillator and hydrogenic approximations.

Figures 3 and 4 give the plots of the average number of phonons around the electron in the GS with α for $\beta = 2$ and $\beta = 10$ respectively. For the same set of α and β, the bound polaron cloud in a quantum well appears to contain a larger number of phonons than in a bulk crystal. This shows that the polaronic effect is stronger in 2D than in 3D.

In figures 5 and 6 we study the variation of the size of the polaron with α for $\beta = 2$ and $\beta = 10$ respectively. For the same values of α and β, the polaron size is smaller in a

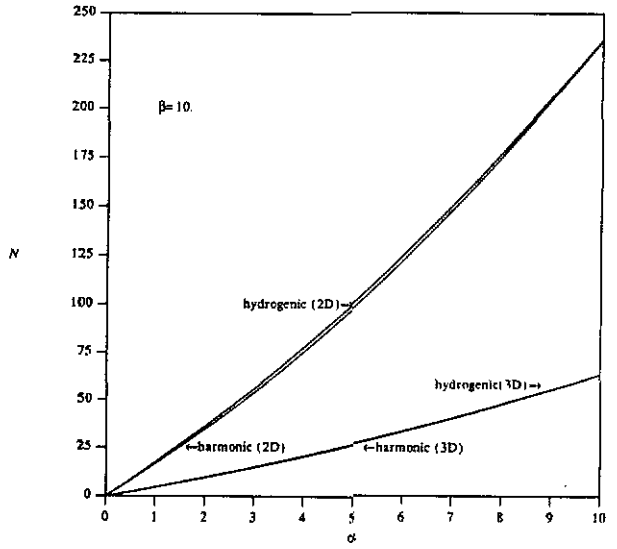

Figure 4. Average number of phonons N around the electron in the GS versus α for $\beta = 10$ in two and three dimensions in harmonic-oscillator and hydrogenic approximations.

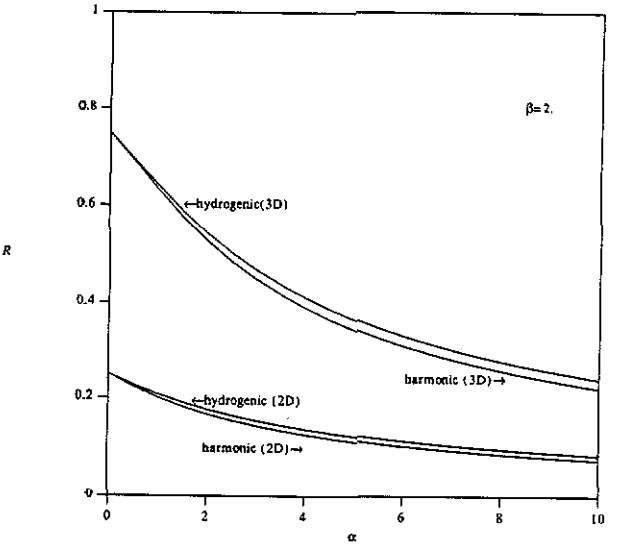

Figure 5. Size of the polaron R (in Feynman units) in the GS versus α for $\beta = 2$ in two and three dimensions in harmonic-oscillator and hydrogenic approximations.

quantum well than in a bulk crystal, which is clearly visible from the figures. This again points to the fact that the polaronic interaction is more pronounced in 2D than in 3D.

To show the efficacy of the LLP-H method we now compare in table 1 the LLP-H values for the GS energy obtained in the harmonic-oscillator approximation with the corresponding Feynman–Haken path-integral results, which we obtain by numerically minimizing equation (24) of [5] with respect to λ. It is clear that the LLP-H results are

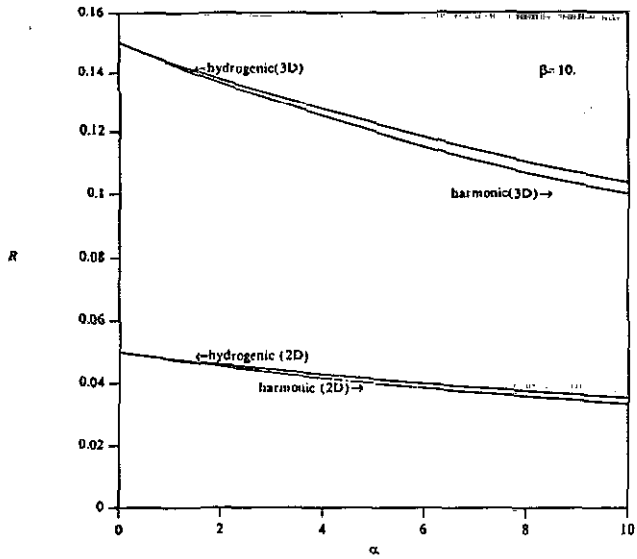

Figure 6. Size of the polaron R (in Feynman units) in the GS versus α for $\beta = 10$ in two and three dimensions in harmonic-oscillator and hydrogenic approximations.

Table 1. The GS energy of the 2D bound polaron in Feynman units. First line: Feynman–Haken path-integral method in the harmonic-oscillator approximation. Second line: LLP-H method in the harmonic-oscillator approximation.

β/α	2	5	10
1	−10.090	−47.642	−173.246
	−9.902	−47.562	−173.202
3	−19.834	−66.69	−207.920
	−19.460	−66.481	−207.80
5	−32.58	−88.822	−245.718
	−32.09	88.522	−245.52
7	−48.402	−114.066	−286.643
	−47.837	−113.69	−286.380
10	−77.966	−157.782	−353.903
	−77.325	−157.316	−353.539

fairly accurate over the entire range of the coupling parameters. (The accuracy of the Feynman–Haken method has already been well established by Matsuura [9] in the context of the bulk problem.) The reason for considering here only the harmonic-oscillator approximation for comparison is that in the Feynman–Haken method this approximation is much easier to handle from the computational point of view.

4. Excited states

For the excited-state energies we employ the hydrogenic approximation and thus use for the first two internal excited states the hydrogenic 2s and 2p wavefunctions:

$$\Phi_{2s} = \frac{4\lambda}{3\sqrt{6}\,\pi}\exp\left(-\frac{2\lambda}{3}\rho\right)\left(1-\frac{4\lambda}{3}\rho\right) \qquad \Phi_{2p} = \frac{8\lambda^2}{9\sqrt{3}\,\pi}\rho\exp\left(-\frac{2\lambda}{3}\rho\right)e^{i\theta} \tag{4.1}$$

with λ as the variational parameter. In the extended- and localized-state limits, we get

ES $$E_{2s} = 2\beta^2/9 - \pi\alpha/2 \qquad E_{2p} = -2\beta^2/9 - \pi\alpha/2 \tag{4.2a}$$

LS $$E_{2s} = -2(\beta/3 + 0.0776\pi\alpha/\sqrt{2})^2 \qquad E_{2p} = -2(\beta/3 + 0.0897\pi\alpha/\sqrt{2})^2. \tag{4.2b}$$

In each of equations (4.2*a*), the first term, i.e. $(-2\beta^2/9)$, may be identified as the degenerate 2s–2p energy of the unperturbed impurity atom in 2D and the second term, i.e. $(-\pi\alpha/2)$, may be regarded as the shift in the impurity atom level due to the electron–SO phonon interaction. This interpretation is, however, strictly perturbative and should not rigorously apply to equations (4.2*a*) because these equations have been derived in the limit $\alpha \to 0, \beta \to 0$, whereas, for the perturbation theory to work rigorously, β should be large and α small. Obviously for equations (4.2*b*) too the perturbative interpretation does not hold in general because here both α and β may be large. But the perturbative interpretation is certainly valid in the following limiting cases:

$$\begin{aligned} E_{2s}(\beta \to \infty, \alpha \to 0) &= -2\beta^2/9 - (0.3104/3\sqrt{2})\,\pi\alpha\beta \\ E_{2p}(\beta \to \infty, \alpha \to 0) &= -2\beta^2/9 - (0.3588/3\sqrt{2})\,\pi\alpha\beta \end{aligned} \tag{4.3}$$

which follow directly from (4.2*b*). We shall however always prefer to use the perturbative language for convenience. Thus we find that, in the case of small α and β, the electron–SO phonon interaction lowers the degenerate 2s and 2p states of the impurity atom by the same amount and hence the degeneracy is not lifted. However when α and β are both large or at least one of them is sufficiently large, the 2p state is lowered more than the 2s level. So in this regime the electron–phonon interaction induces a splitting in the 2s–2p levels of the impurity atom, leading to the so-called phonon Lamb shift.

For intermediate values of the coupling parameters the calculation has been done numerically. The variation of the 2s and 2p energies with α has been studied for two values of β ($\beta = 2$, $\beta = 10$). The results are shown graphically in figures 7 and 8. It is clear that for $\beta = 2$ (figure 7) the 2s and 2p states have the same energy up to large enough α (say $\alpha = 10$), while for $\beta = 10$ (figure 8) the 2s–2p degeneracy is lifted even at much smaller values of α. One may also notice that the phonon-induced Lamb shift $(E_{2p} - E_{2s})$ increases with increasing α.

In table 2 we present the 1s, 2s and 2p energies, 1s–2s and 1s–2p transition energies and the phonon Lamb shifts for a number of polar materials. The phonon Lamb shift is found to be zero for GaAs, ZnAs, CdS, ZnO, MnO and TiCl; while for the alkali halides like NaCl, KCl, NaBr, NaI and KI and for Cu_2O, the 2p states are found to have much lower energies than the 2s states and consequently large phonon Lamb shifts are predicted for these materials. For all the above materials we have also performed a 3D calculation for the sake of comparison (table 3). It may be noted that for the bulk crystals of the alkali halides the Lamb shifts are of much smaller magnitude compared to the corresponding quantum-well values, and in bulk Cu_2O the Lamb shift is zero. Furthermore, the sign of the shift in the 2D alkali halides is opposite to that in the bulk cases. This phenomenon of reversal in the sign of the phonon Lamb shift that we find for the same material as we go from its bulk crystalline form to the 2D quantum-well structure is indeed an interesting theoretical observation and should be tested experimentally. Such investigations might be important in completely different contexts

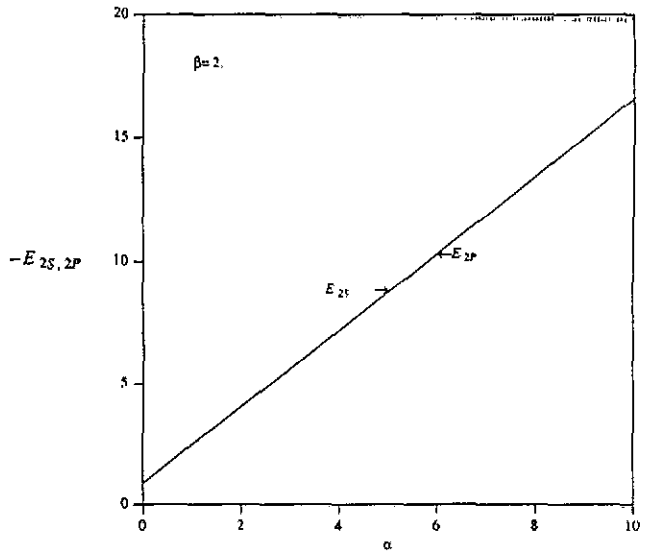

Figure 7. The 2D bound-polaron excited-state energies E_{2s} and E_{2p} (in Feynman units) versus α for $\beta = 2$ in the hydrogenic approximation.

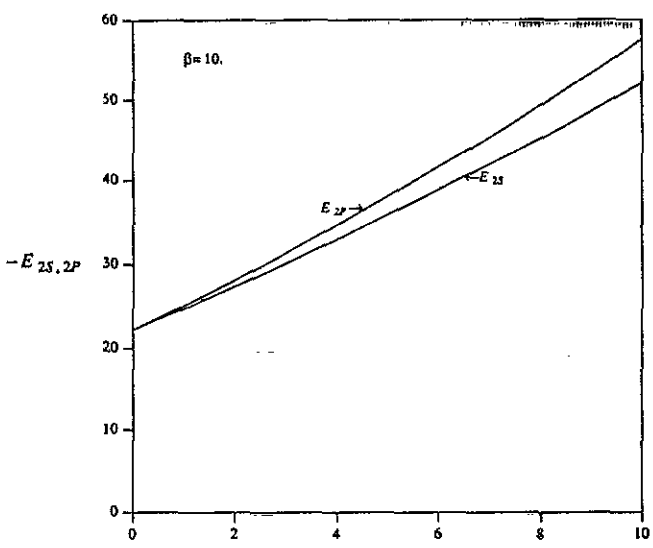

Figure 8. The 2D bound-polaron excited-state energies E_{2s} and E_{2p} (in Feynman units) versus α for $\beta = 10$ in the hydrogenic approximation.

as well. For instance, a similar analysis on CuO_2-based high-T_c materials might by useful in dictating whether polaronic interactions are present at all in these materials and, if they are, whether they are in the CuO_2 plane only or they also have a sizable component along the c axis.

Table 2. The LLP-H results for GS energies (E_{1s}), excited-state energies (E_{2s}, E_{2p}), transition energies ($E_{1s} - E_{2s}$, $E_{1s} - E_{2p}$) and Lamb shift corrections ($E_{2p} - E_{2s}$) in meV for the 2D bound polaron in the hydrogenic approximation for a few polar materials. The values for $\hbar\omega_s$ have been calculated using the relation $\hbar\omega_s = \hbar\omega_B[\varepsilon_\infty(\varepsilon_0 + 1)/\varepsilon_0(\varepsilon_\infty + 1)]^{1/2}$, where ω_B is the bulk optical-phonon frequency. The values of ε_0, ε_∞, m/m_e (m = band mass, m_e = bare electron mass) and $\hbar\omega_B$ for GaAs to TiCl have been taken from the second of [3] and for NaCl to Cu_2O from [9].

Materials	ε_0	ε_∞	$\hbar\omega_s$	m/m_e	α	β	E_{1s}	E_{2s}	E_{2p}	$E_{1s} - E_{2s}$	$E_{1s} - E_{2p}$	$E_{2p} - E_{2s}$
GaAs	12.8	10.9	36.4	0.066	0.116	1.01	−82.7	−14.9	−14.9	−67.8	−67.8	0
ZnS	8.7	5.2	42.2	0.19	0.9	2.26	−594.9	−109.3	−109.3	−485.6	−485.60	0
CdS	8.8	5.2	36.5	0.18	0.98	2.33	−553.8	−100.9	−100.9	−452.9	−452.9	0
ZnO	8.84	4.00	67.94	0.28	1.47	2.15	−1044.0	−226.98	−226.98	−817.02	−817.02	0
MnO	9.80	2.97	81.72	0.25	2.05	1.68	−1065	−315.02	−315.02	−749.98	−749.98	0
TiCl	37.6	5.1	19.92	0.37	4.38	1.16	−360.42	−143.13	−143.14	−217.29	−217.28	0.01
NaCl	5.62	2.25	3.11	2.8	11.3	15.47	−23739	−2964	−3222	−20775	−20517	−258
KCl	4.68	2.13	2.2	1.85	9.7	16.8	−20169	−2468.8	−2648.2	−17700.3	−17520.8	−179.5
NaBr	5.99	2.6	23.2	2.96	11.1	16.9	−21547.9	−2663.6	−2878	−18884.3	−18669.9	−214.41
NaI	6.60	2.9	20.15	3.25	11.6	17.4	−19973	−2471	−2672	−17502	−17301	−201
KI	4.9	2.7	16.96	2.1	8.4	19.4	−17793.2	−2133.2	−2256.3	−15659.96	−15536.8	−123.1
Cu_2O	10.5	4	49.9	1.8	5.08	5.5	−5825.2	−794.7	−858.5	−5030.5	−4966.6	−63.9

Table 3. The LLP-H results for GS energies ($E_{1s} = E_{LLP\text{-}H}$), excited-state energies (E_{2s}, E_{2p}), transition energies ($E_{1s} - E_{2s}$, $E_{1s} - E_{2p}$) and Lamb shift corrections ($E_{2p} - E_{2s}$) in meV for the 3D bound polaron in the hydrogenic approximation for a few polar materials. The material parameters have been taken from the sources referred to in table 2.

Materials	ε_0	ε_∞	m/m_e	$\hbar\omega_B$	α	β	E_{1s}	E_{2s}	E_{2p}	$E_{1s} - E_{2s}$	$E_{1s} - E_{2p}$	$E_{2p} - E_{2s}$
GaAs	12.83	10.90	0.066	36.7	0.068	0.543	−7.89	−3.848	−3.848	−4.042	−4.042	0
ZnS	8.77	5.20	0.19	43.7	0.602	1.24	−59.90	−34.707	−34.707	−25.193	−25.193	0
CdS	8.90	5.2	0.18	37.8	0.643	1.28	−55.27	−32.047	−32.047	−23.223	−23.223	0
ZnO	8.84	4	0.28	72.0	0.995	1.163	−120.33	−83.81	−83.81	−36.52	−36.52	0
MnO	9.80	2.97	0.25	90.0	1.44	0.885	−164.84	−138.81	−138.81	−26.03	−26.03	0
TiCl	37.6	5.10	0.37	21.5	2.59	0.575	−59.23	−56.57	−56.57	−2.66	−2.66	0
NaCl	5.62	2.25	2.78	32.234	9.17	8.6	−2609.7	−673.3	−662.7	−1936.4	−1947	10.6
KCl	4.68	2.13	1.8	25.46	7.6	9	−1949.7	−502.13	−494.15	−1447.6	−1455.5	7.9
NaBr	5.99	2.62	2.96	25.26	8.6	9.45	−2222.3	−568.7	−563	−1653.6	−1659.3	5.7
NaI	6.60	2.91	3.25	21.77	8.653	9.65	−1979.96	−505.69	−501.50	−1474.27	−1478.5	4.23
KI	4.94	2.69	2.11	18.11	6.682	11.30	−1841.76	−465.87	−464.637	−1375.89	−1377.12	1.23
Cu_2O	10.5	4	1.81	53.28	3.363	2.927	531.11	−236.24	−236.24	−294.87	−294.87	0

5. Conclusions

In conclusion, the bound-polaron problem in a purely 2D quantum well has been investigated for the entire range of the electron–phonon coupling constant α and the Coulomb binding parameter β using the LLP-H method. The GS energy, the mean number of phonons in the polaron cloud and the size of the polaron are obtained in both harmonic-oscillator and hydrogenic approximations. The GS energy values have also been computed for a number of polar materials. Comparison of the LLP-H energies (in the harmonic-oscillator approximation) with the corresponding Feynman–Haken path-integral results shows that the LLP-H method is fairly accurate over the entire range of α and β. We find from our LLP-H calculation that, when α and β are both large or both small or α is small and β large, the hydrogenic trial function proves to be a better choice as the electronic function, while for the case of sufficiently large α and small β the harmonic-oscillator approximation seems to provide a better description of the situation. A comparison of the 2D GS properties with the corresponding 3D ones shows that the polaronic effects are stronger in quantum wells than in bulk materials. The scaling relation between the 2D and 3D bound-polaron GS energies, which was proposed recently by Bhattacharya *et al* [5] in the harmonic-oscillator approximation, is found to be satisfied for all α and β.

Though from the point of view of accuracy the Feynman–Haken path-integral method looks somewhat better, the LLP-H scheme has an important advantage in that it can be easily applied to the excited states. We have obtained the 2s and 2p excited-state energies of the 2D bound polaron in the hydrogenic approximation. It is observed that in the case of small α and β, the 2s–2p degeneracy of the hydrogenic impurity is not lifted, while in the case of large α and β (or large β and small α), the degenerate 2s–2p levels do split, leading to the phonon Lamb shift. For a number of materials we have found that the 2D phonon Lamb shifts are much larger than the corresponding 3D ones and are of opposite sign. This, as we have already mentioned, is an interesting theoretical observation and should show up in the optical absorption experiments on hydrogen-doped thin films of some ionic materials. Our analysis is, however, based on a purely 2D model, which is an idealized model, and a realistic calculation should use a quasi-2D model. Such investigations are in progress and the results will be reported in due course.

Acknowledgment

Part of this work was done when one of the authors (AC) was at the S N Bose National Centre for Basic Sciences, Calcutta, India.

References

[1] Bhattacharya M, Mukhopadhyay S and Mitra T K 1987 *Phys. Status Solidi* b **142** 141
Das Sarma S 1984 *Surf. Sci.* **142** 341
Xiaoguang Wu, Peeters F M and Devreese J T 1985 *Phys. Rev.* B **31** 3420
[2] Bhattacharya M, Mukhopadhyay S and Mitra T K 1983 *Phys. Status Solidi* b **120** 555
[3] Zheng R S, Gu S W and Lin D L 1986 *Solid State Commun.* **59** 331
Gu S W and Zheng R S 1987 *Solid State Commun.* **62** 695; 1987 *Phys. Rev.* B **36** 3280
Zheng L F, Li Y C and Gu S W 1988 *J. Phys. C: Solid State Phys.* **21** 3047
[4] Mason B A and Das Sarma S 1986 *Phys. Rev.* B **33** 8379

[5] Bhattacharya M, Chatterjee A and Mitra T K 1989 *Phys. Rev.* B **39** 8351
[6] Lee T D, Low F E and Pines D 1953 *Phys. Rev.* **90** 297
[7] Huybrechts W 1977 *J. Phys. C: Solid State Phys.* **10** 3761
[8] Platzman P M 1962 *Phys. Rev.* **125** 1961
[9] Matsuura M 1974 *Can. J. Phys.* **52** 1